Transport of Finite-Sized Particles in Chaotic Flow

Nicholas T. Ouellette,[1,*] P. J. J. O'Malley,[1] and J. P. Gollub[1,2,+]

[1]Department of Physics, Haverford College, Haverford, Pennsylvania 19041, USA
[2]Department of Physics, University of Pennsylvania, Philadelphia, Pennsylvania 19014, USA

(Received 26 June 2008; published 24 October 2008)

By extending traditional particle tracking techniques, we study the dynamics of neutrally buoyant finite-sized particles in a spatiotemporally chaotic flow. We simultaneously measure the flow field and the trajectories of millimeter-scale particles so that the two can be directly compared. While the single-point statistics of the particles are indistinguishable from the flow statistics, the particles often move in directions that are systematically different from the underlying flow. These differences are especially evident when Lagrangian statistics are considered.

DOI: 10.1103/PhysRevLett.101.174504 PACS numbers: 47.55.Kf, 47.80.Jk

Understanding the dynamics of transported particulate matter in fluid flows is a longstanding problem with wide applicability. In nature, for example, plant spores and pathogens are carried by atmospheric flow [1]. Clouds are suspensions of water droplets in turbulent air [2,3]. Fuel injectors transport droplets at supersonic speeds [4]. In addition, many modern flow measurement techniques, including laser doppler anemometry, particle image velocimetry, and particle tracking schemes require seeding the flow with particles.

When the particles are very small, spherical, and neutrally buoyant, they behave as infinitesimal fluid elements. In this limit, significant progress has been made in understanding their behavior during the past decade [5,6]. When these conditions are not met, however, the particles may no longer follow the flow. Instead, they behave as if they have inertia relative to the carrier flow, responding to changes in the underlying flow field only over a finite time. This lagging effect is evident, for example, in the reduction of the acceleration variance for such inertial particles in turbulence [7–10]. Inertial particles have also been shown to accumulate in particular regions of the flow: particles denser than their carrier flow, for example, are ejected from vortices and therefore congregate in regions of high strain [11–15]. This preferential concentration leads to an apparent clustering effect that is key, for example, in understanding the initiation of rainfall in warm clouds [2,3].

Particles may behave inertially and fail to follow the flow for two reasons. If they have a density different from the carrier flow, they take a finite time to respond to flow accelerations. Even if they are neutrally buoyant, however, particles of finite size can behave inertially since the flow stresses are averaged over the particle surface [10,16,17]. The latter case has implications for flow measurements: simply choosing particles of the same density as the fluid does not imply that the particles will faithfully follow the flow. The importance of both size and density are thought to be captured by the Stokes number, the nondimensional coefficient of the viscous drag term in the particle equation of motion [18]. The Stokes number, defined as

$$\mathrm{St} = \frac{2}{9}\frac{\rho_p}{\rho_f}\left(\frac{a}{L}\right)^2 \mathrm{Re}, \tag{1}$$

where ρ_p and ρ_f are the particle and fluid densities, respectively, a is the particle radius, L is the characteristic flow length scale, and Re is the Reynolds number of the carrier flow, is high for dense or large particles or for strong flow driving. In this Letter, we study the dynamics of neutrally buoyant large particles in a quasi-two-dimensional laboratory flow. In addition to the large particles, we also simultaneously measure the dynamics of very small tracer particles that we assume to follow the flow to a good approximation, in order to compare the inertial particles and the flow field directly. Though the Stokes numbers of our inertial particles are relatively small, we observe measurable inertial effects, particularly for time-resolved statistics.

Particles whose inertia comes purely from finite-size effects are less well studied than their heavy counterparts [10,16,17]. In numerical simulations, for example, it is simpler to study a pointlike, heavy particle than to simulate a large particle accurately, which would require solving the Navier-Stokes equations along the particle surface. Simulations also typically neglect some of the more complex terms in the particle equation of motion [18], particularly the Bassett history force, even though these terms may in some situations be significant [19]. Experiments, of course, do not have these difficulties, but have provided limited information since they have not previously had access to the underlying flow field. Ours is the first experiment to provide the velocity field and inertial particle information simultaneously.

We generate quasi-2D flow by driving a thin layer of an electrolytic fluid electromagnetically [20]. A 3.5-mm-deep layer of 17% KCl in water lies above a square lattice of permanent magnets with alternating polarity; when a current is driven across the fluid, Lorentz forces set it into motion. The Reynolds number is given by $\mathrm{Re} = UL/\nu$,

where U is the root-mean-square velocity, $L = 2.54$ cm is the magnet spacing, and ν is the kinematic viscosity. In our experiments, $72 \leq \mathrm{Re} \leq 220$, which is above the transition to spatiotemporal chaos for this flow [21]. As shown in Fig. 1, the flow contains three sizes of neutrally buoyant polystyrene particles. The smallest are 80 μm in diameter, with $1.6 \times 10^{-4} \leq \mathrm{St} \leq 4.5 \times 10^{-4}$; we therefore expect them to follow the flow well. The larger particles have diameters of $d = 0.92$ mm $(0.53 \times 10^{-2} \leq \mathrm{St} \leq 1.6 \times 10^{-2})$ and $d = 2.00$ mm $(2.5 \times 10^{-2} \leq \mathrm{St} \leq 7.6 \times 10^{-2})$. All three sizes of particles are non-Brownian. The particles are slightly polydisperse: the standard deviation of the diameter for the $d = 0.92$ mm particles is $\sigma = 0.07$ mm, while $\sigma = 0.01$ mm for the $d = 2.00$ mm particles. To avoid any surface-tension-driven interactions between the particles [22], we place a 3.5-mm-deep layer of water above the salt solution; the particles lie at the interface between the electrolyte and the water. Since the two layers are miscible, there is no bulk surface tension between them. By keeping the loading density of the large particles low (see Fig. 1), we reduce the possibility of particle collisions or other particle-particle interactions. We image the particles at a rate of 30 Hz and with a precision of approximately 13 μm (0.1 pixels); to avoid boundary effects, we focus on a 7.5 cm $\times$ 7.5 cm region in the center of the flow. Using tracking software [23], we determine the trajectories of the three types of particles independently; their velocities and accelerations are then measured by fitting polynomials to short segments of the trajectories [24]. In order to resolve the velocity field well, there are roughly 15 000 tracers in the measurement area at any time. Even with this loading density, we calculate that interactions between the tracer particles are generally negligible.

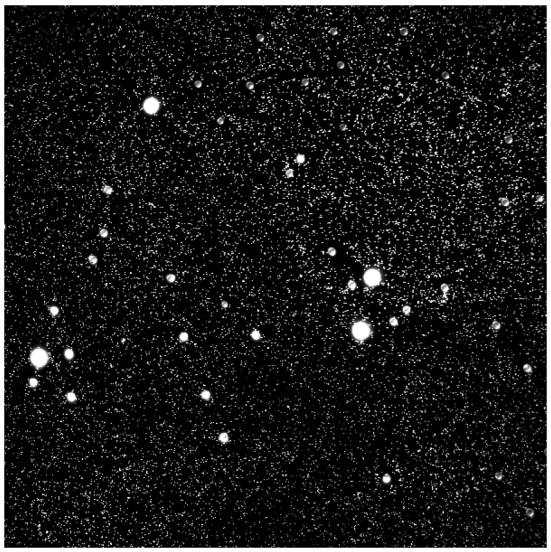

FIG. 1. Sample image from our experiment. The three sizes of particles are easily distinguishable by our particle identification algorithms. The contrast of this image has been enhanced to show the tracer particles more clearly.

As mentioned above, our flow is not turbulent, even though the carrier flows studied both in simulation [8,13,14] and experiment [9–11,15] are typically turbulent. In previous work, the particle size is typically assumed to be smaller than the Kolmogorov length scale. In this limit, the local flow around the particles is random but smooth, just as it is for our flow. Our results should therefore have relevance for turbulent particle-laden flows. Additionally, inertial effects have previously been seen in simulation for spatiotemporally chaotic flows like ours [16,17,25].

For particles with $\mathrm{St} > 0.1$, previous studies have found that the acceleration statistics of inertial particles differ from those of fluid elements, for both heavy [8,9] and large particles [7,10]. In each case, the acceleration variance decreased as the Stokes number increased; for the heavy particles, the acceleration probability density function (PDF) also became narrower for higher St. In Fig. 2, we show both the velocity and acceleration PDFs for our particles. Surprisingly, we find no statistically significant, systematic difference between the single-point velocity or acceleration of the three different sizes for any Re tested. We find similar results for the vorticity or strain rate seen by the three sizes of particles. These results suggest that particles with $\mathrm{St} \sim \mathcal{O}(10^{-2})$ are good flow tracers if only the single-point flow statistics are desired.

Closer investigation of the particle dynamics, however, reveals differences between the large particles and the

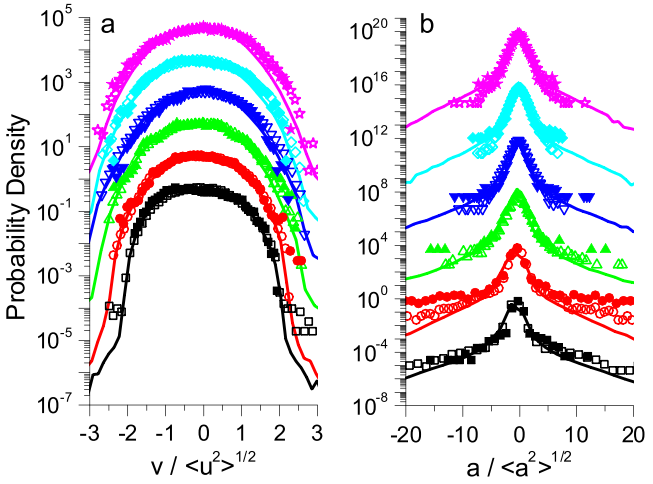

FIG. 2 (color online). Probability density functions (PDFs) of (a) the particle velocity and (b) acceleration. The PDFs for different Reynolds numbers have been offset for clarity: from bottom to top, Re = 72 (■), 108 (●), 155 (▲), 185 (▼), 208 (◆), and 220 (★). The velocities and accelerations have been normalized by the root-mean-square values measured from the tracer particles. Solid lines show data for the $d = 80$ μm tracers, open symbols for the $d = 0.92$ mm particles, and solid symbols for the $d = 2.00$ mm particles. There is no statistically significant difference between the three particle sizes.

tracers. Since we have access to the fluid velocity field $\mathbf{u}$ as well as the velocities $\mathbf{v}$ of the large particles, we can directly compare the two. Let us define the vector velocity difference $\mathbf{w} = \mathbf{v} - \mathbf{u}$. In Fig. 3, we show the PDF of $|\mathbf{w}|$ for all three sizes of particles. We note that $\mathbf{w}$ is not strictly zero even for the tracer particles, due to smoothing of the measured velocity field and errors introduced by numerical interpolation when comparing the particle and fluid velocities [26]; the tracer PDFs therefore give the baseline accuracy of our measurements. We find a systematic trend for the inertial particles: larger particles are more likely to differ in velocity from the underlying flow field, even though St is small. We also show in Fig. 3 the PDFs of the two ingredients of $\mathbf{w}$: the difference in speed $\delta v = |\mathbf{v}| - |\mathbf{u}|$ and the angle θ between $\mathbf{v}$ and $\mathbf{u}$. From Fig. 3(b), we see that the large particles may move both faster and slower than the underlying flow; indeed, the PDFs are surprisingly skewed towards the fast side for the large particles. Systematic growth of the speed difference δv with increasing particle size is not clearly evident from our data, particularly for the slow side of the PDF. On the other hand, from Fig. 3(c), we see that larger particles are systematically more likely to be moving in a direction different from the fluid element at the same location.

In addition to these single-time statistics, our measurements allow us to study the time dependence of inertial effects. We directly measure the trajectories of the large particles. Our velocity fields are resolved in time; we can therefore create trajectories of virtual ideal fluid elements by integrating the velocity fields in time [20,24,27,28]. By choosing the initial positions of these virtual particles to coincide with measured positions of the large particles, we can compare the trajectories of inertial particles and fluid elements directly. We show samples of these virtual trajectories along with their parent physical trajectories in Figs. 4(a) and 4(b). As shown in Fig. 4(a), the large particles sometimes follow the fluid very well. As shown in Fig. 4(b), however, the virtual trajectories sometimes separate from their parent tracks wildly; empirically, we observe such strong separations near hyperbolic points [21]. To quantify this effect, we have measured the growth of the mean-squared distance between the physical and virtual trajectories, as shown in Fig. 4(c). For the tracer particles, we see roughly exponential growth of the mean-squared separation in time, as is expected for a chaotic flow: the finite resolution with which we locate the physical particles leads to slightly different initial conditions for the physical and virtual trajectories. The mean-squared separation for the large particles, however, grows approximately as a t^2 power law. We also find that the virtual particles separate systematically faster from the larger of the inertial particles: the scaling exponent is roughly the same, but the coefficient is larger, as shown in Figs. 4(d) and 4(e).

Our results clearly show that the large particles behave inertially, even though St is small; the effects we see, however, do not scale with St as it is defined in Eq. (1). In Fig. 3, for example, the difference between the $d = 0.92$ mm and $d = 2.00$ mm particles is clearly evident; there are, however, no systematic differences between the data for different Re, even though we expect that St $\sim$ Re. A similar trend is seen in Fig. 4(c): since St for the $d = 0.92$ mm particles at our *highest* Re is smaller than St for the $d = 2.00$ mm particles at our *lowest* Re, we would expect that all the $d = 2.00$ mm curves should lie above the $d = 0.92$ mm curves. By fitting the mean-squared displacement curves to t^2 power laws and extracting the coefficient D, we show in Fig. 4(d) that this is not the case: the data for the two sizes of particles as a function of St do not lie on a single curve. Nevertheless, at each Re, the $d = 2.00$ mm particles have larger values of D than their $d = 0.92$ mm counterparts do, as shown in Fig. 4(e). Our data therefore suggest that the Stokes number as defined in Eq. (1) does not fully account for the effects of particle

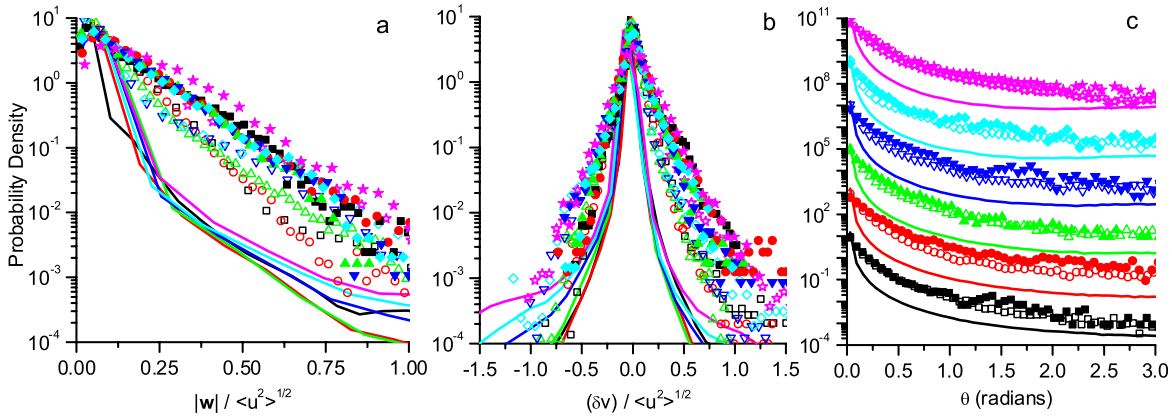

FIG. 3 (color online). PDFs of (a) the magnitude of the vector velocity difference between the particle and the flow $|\mathbf{w}|$, (b) the speed difference δv, and (c) the angle between the particle velocity vector and the flow velocity vector θ, with the θ PDFs offset for clarity. The symbols are the same as in Fig. 2. The tracer data (solid lines) show our baseline accuracy. For $|\mathbf{w}|$ and θ, the $d = 2.00$ mm particles deviate from the flow systematically more than the $d = 0.92$ mm particles. For δv, the trend is unclear.

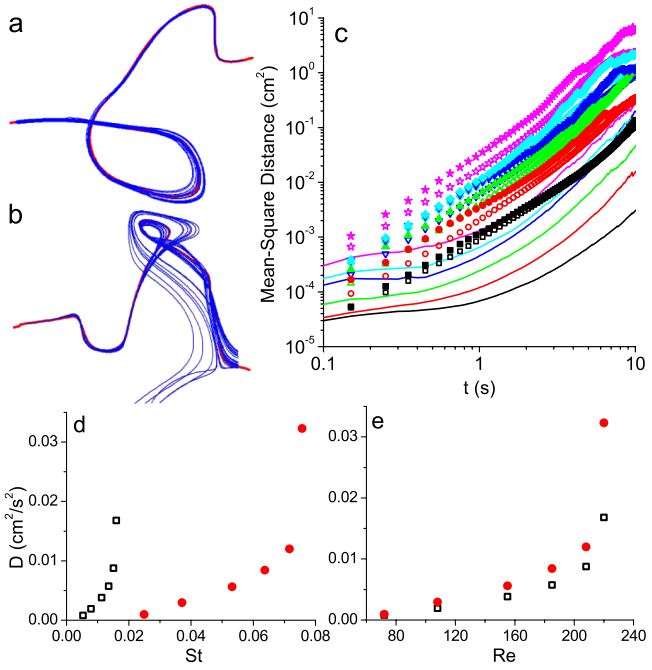

FIG. 4 (color online). (a),(b) Sample physical and virtual trajectories for the $d = 2.00$ mm particles. Physical trajectories are shown as thick lines (red online), and virtual trajectories as thin lines (blue online). The large particles sometimes track the flow nearly perfectly (a), and sometimes deviate wildly (b). (c) Evolution of the mean-squared distance between a physical particle and a virtual particle with identical initial conditions. Symbols are the same as in Fig. 2, and solid lines represent the tracers. (d),(e) Coefficients of t^2 power-law fits to the mean-squared distance (relative to the virtual particles) for the two sizes of inertial particles. Squares show the $d = 0.92$ mm particle data, and circles the $d = 2.00$ mm particle data. No clear trend is seen as a function of St (d), but the $d = 2.00$ mm particles separate faster than their $d = 0.92$ mm counterparts at each Re (e).

inertia. Our data are not simply a function of either St or Re alone.

Taken together, our results suggest that Lagrangian measurements following the trajectories of particles are more sensitive to inertial effects: the single-point statistics of the large particles shown in Fig. 2 are indistinguishable from their tracer counterparts, but, as shown in Fig. 4, the effects of even a small amount of particle inertia are very clear over long times. From Fig. 3, it appears that the main consequence of the inertia of large particles is to produce misalignment of the particle and flow velocities. Finally, we find that the inertial effects do not scale with the Stokes number as usually defined. Our results indicate that work remains to be done in understanding the dynamics of inertial particles.

We thank Z. Warhaft for helpful discussions. This work was supported by the National Science Foundation under Grants No. DMR-0405187 and No. DMR-0803153.

*Present address: Department of Mechanical Engineering, Yale University, New Haven, CT 06520, USA.
+jgollub@haverford.edu

[1] J. K. M. Brown and M. S. Hovmøller, Science **297**, 537 (2002).
[2] G. Falkovich, A. Fouxon, and M. G. Stepanov, Nature (London) **419**, 151 (2002).
[3] R. A. Shaw, Annu. Rev. Fluid Mech. **35**, 183 (2003).
[4] A. G. MacPhee *et al.*, Science **295**, 1261 (2002).
[5] G. Falkovich, K. Gawędzki, and M. Vergassola, Rev. Mod. Phys. **73**, 913 (2001).
[6] P. K. Yeung, Annu. Rev. Fluid Mech. **34**, 115 (2002).
[7] G. A. Voth, A. La Porta, A. M. Crawford, J. Alexander, and E. Bodenschatz, J. Fluid Mech. **469**, 121 (2002).
[8] J. Bec *et al.*, J. Fluid Mech. **550**, 349 (2006).
[9] S. Ayyalasomayajula, A. Gylfason, L. R. Collins, E. Bodenschatz, and Z. Warhaft, Phys. Rev. Lett. **97**, 144507 (2006).
[10] N. M. Qureshi, M. Bourgoin, C. Baudet, A. Cartellier, and Y. Gagne, Phys. Rev. Lett. **99**, 184502 (2007).
[11] K. D. Squires and J. K. Eaton, Phys. Fluids A **3**, 1169 (1991).
[12] J. K. Eaton and J. R. Fessler, Int. J. Multiphase Flow **20**, 169 (1994).
[13] J. Bec, A. Celani, M. Cencini, and S. Musacchio, Phys. Fluids **17**, 073301 (2005).
[14] J. Chun, D. L. Koch, S. L. Rani, A. Ahluwalia, and L. R. Collins, J. Fluid Mech. **536**, 219 (2005).
[15] E. W. Saw, R. A. Shaw, S. Ayyalasomayajula, P. Y. Chuang, and A. Gylfason, Phys. Rev. Lett. **100**, 214501 (2008).
[16] A. Babiano, J. H. E. Cartwright, O. Piro, and A. Provenzale, Phys. Rev. Lett. **84**, 5764 (2000).
[17] T. Sapsis and G. Haller, Phys. Fluids **20**, 017102 (2008).
[18] M. R. Maxey and J. J. Riley, Phys. Fluids **26**, 883 (1983).
[19] R. J. Hill, Phys. Fluids **17**, 037103 (2005).
[20] M.-C. Jullien, J. Paret, and P. Tabeling, Phys. Rev. Lett. **82**, 2872 (1999).
[21] N. T. Ouellette and J. P. Gollub, Phys. Rev. Lett. **99**, 194502 (2007).
[22] D. Vella and L. Mahadevan, Am. J. Phys. **73**, 817 (2005).
[23] N. T. Ouellette, H. Xu, and E. Bodenschatz, Exp. Fluids **40**, 301 (2006).
[24] G. A. Voth, G. Haller, and J. P. Gollub, Phys. Rev. Lett. **88**, 254501 (2002).
[25] I. J. Benczik, Z. Toroczkai, and T. Tél, Phys. Rev. Lett. **89**, 164501 (2002).
[26] We smooth the velocity fields using a boxcar average of width $L/10$. We use bilinear interpolation to obtain the flow velocity away from the grid points. We also tested cubic spline and quintic polynomial interpolation, with no noticeable gains in accuracy.
[27] M. K. Rivera and R. E. Ecke, Phys. Rev. Lett. **95**, 194503 (2005).
[28] We use a second-order Runge-Kutta integrator to create the virtual trajectories. Higher-order integration schemes did not noticeably alter the results.